Supporting Information

Excimer-induced high-efficiency fluorescence due to pairwise anthracene stacking in crystal with long lifetime

Haichao Liu,[a] Liang Yao,[a] Bao Li,[a] Xiankai Chen,[b] Yu Gao,[a] Shitong Zhang,[a] Weijun Li,[c] Ping Lu,[a] Bing Yang,*[a] Yuguang Ma[d]

[a] State Key Laboratory of Supramolecular Structure and Materials, Jilin University, Changchun, 130012, P. R. China

[b] College of Chemistry, Jilin University, Changchun, 130012, P. R. China

[c] College of Chemical Engineering, Zhejiang University of Technology, Hangzhou, 310014, P. R. China

[d] State Key Laboratory of Luminescent Materials and Devices, South China University of Technology, Guangzhou, 510640, P. R. China

*Corresponding Author. E-mail: yangbing@jlu.edu.cn

Contents

SI The details of synthetic procedures

SI-1 General information: All the reagents and solvents used for the synthesis were purchased from Aldrich and Acros companies and used without further purification. The synthesis procedure was presented in Scheme S1. ^{1}H and ^{13}C NMR spectra were recorded on a Bruker AVANCE 500 spectrometer at 500 MHz, using tetramethylsilane (TMS) as the internal standard. The MALDI-TOF-MS mass spectra were recorded using an AXIMA-CFR^{TM} plus instrument. The compounds were characterized by a Flash EA 1112, CHNS elemental analysis instrument.

SI-2 The synthesis of 2-(anthracen-9-yl)thianthrene (2-TA-AN)

2-bromothianthrene (2-Br-TA)

The synthesis of 2-Br-TA was referring to Ref. 1.[1]

4,4,5,5-tetramethyl-2-(thianthren-2-yl)-1,3,2-dioxaborolane (2-B-TA)

A mixture of 2-Br-TA (2.80 g, 9.5 mmol), bis(pinacolato)diboron (2.54 g, 10 mmol), $PdCl_2$(dppf) (155 mg, 0.19 mmol), KOAc (4.66 g, 47.5 mmol) and 40 ml 1, 4-dioxane was degassed and recharged with nitrogen. After stirred and refluxed at 85 ℃ for 48 h under nitrogen atmosphere, the mixture was washed with distilled water and then extracted with dichloromethane. The organic phase was dried with anhydrous sodium sulfate, filtered and concentrated in vacuum. It was purified via silica gel chromatography by the mixture of petroleum ether/dichloromethane (3:1) to afford the desired compound in 70% yield (2.16 g). ^{1}H NMR (500 MHz, DMSO, 25 ℃, TMS): δ =7.75 (s, 1H), 7.61 – 7.56 (m, 4H), 7.38 – 7.35 (m, 2H), 1.29 (s, 12H). MALDI-TOF MS (mass *m/z*): 342.28 [M^+].

2-(anthracen-9-yl)thianthrene (2-TA-AN)

A mixture of 2-B-TA (900 mg, 2.63 mmol), 9-bromoanthracene (720 mg, 2.80 mmol), K_2CO_3 (3.31 g, 24 mmol), 8 mL distilled water, 12 mL toluene and 6 mL anhydrous ethanol was degassed and recharged with nitrogen. Then $Pd(PPh_3)_4$ (65 mg, 0.056 mmol) was added in the mixture as catalyst, and the mixture was degassed and recharged with nitrogen again. After stirred and refluxed at 90℃ for 48 h under nitrogen atmosphere, the mixture was extracted with dichloromethane. The organic phase was dried with anhydrous sodium sulfate, filtered and concentrated in vacuum. It was purified via silica gel chromatography by the mixture of petroleum ether/dichloromethane (10:1) to afford the desired compound in 76% yield (840 mg). The product was further purified by sublimation. ^{1}H NMR (500 MHz, DMSO, 25 ℃, TMS): δ =8.72 (s, 1H), 8.17 (d, *J* = 8.5 Hz, 2H), 7.84 (d, *J* = 7.9 Hz, 1H), 7.72 – 7.67 (m, 1H), 7.66 – 7.61 (m, 2H), 7.53 (dd, *J* = 15.8, 7.5 Hz, 4H), 7.46 – 7.37 (m, 5H); ^{13}C NMR (500 MHz, $CDCl_3$, 25 ℃, TMS): δ = 138.697 (C), 135.854 (C), 135.592 (C), 135.561 (C), 135.144 (C), 134.703 (C), 131.303 (C), 131.194 (CH), 130.741 (CH), 130.124 (C), 128.902 (CH), 128.831 (CH), 128.574 (CH), 128.406 (CH), 127.835 (CH), 127.821 (CH), 127.054 (CH), 126.507 (CH), 125.662 (CH), 125.195 (CH); MALDI-TOF MS (mass *m/z*): 392.07 [M^+]. Anal. calcd for $C_{26}H_{16}S_2$: C 79.55, H 4.11, S 16.34; found: C 79.84, H 4.09, S 16.58.

SI-3 The synthesis of 1-(anthracen-9-yl)thianthrene (1-TA-AN)

A mixture of thianthren-1-ylboronic acid (1.04 g, 4.0 mmol), 9-bromoanthracene (1.03 g, 4.0 mmol), K_2CO_3 (3.31 g, 24.0 mmol), 8 mL distilled water, 12 mL toluene and 6 mL anhydrous ethanol was degassed and recharged with nitrogen. Then $Pd(PPh_3)_4$ (92 mg, 0.08 mmol) was added in the mixture as catalyst, and the mixture was degassed and recharged with nitrogen again. After stirred and refluxed at 90℃ for 48 h under nitrogen atmosphere, the mixture was extracted with dichloromethane. The organic phase was dried with anhydrous sodium sulfate, filtered and concentrated in vacuum. It was purified via silica gel chromatography by the mixture of petroleum ether/dichloromethane (5:1) to afford the desired compound in 90% yield (1.40 g). The product was further purified by sublimation. ^{1}H NMR (500 MHz, DMSO, 25 ℃, TMS): δ = 8.78 (s, 1H), 8.22 (d, *J* = 8.5 Hz, 2H), 7.82 (dd, *J* = 7.8, 1.2 Hz, 1H), 7.63 – 7.52 (m, 4H), 7.43 (dd, *J* = 8.2, 7.1 Hz, 2H), 7.37 (dd, *J* = 7.4, 1.2 Hz, 1H), 7.35 – 7.29 (m, 3H), 7.20 – 7.13 (m, 1H), 7.02 (d, *J* = 6.8 Hz, 1H); ^{13}C NMR (500 MHz, $CDCl_3$, 25 ℃, TMS): δ = 138.613 (C), 137.442 (C), 136.073 (C), 135.988 (C), 135.803 (C), 134.196 (C), 131.345 (C), 130.981 (CH), 130.081 (C), 128.896 (CH), 128.573 (CH), 128.365 (CH), 127.562 (CH), 127.531 (CH), 127.416 (CH), 127.295 (CH), 126.271 (CH), 125.886 (CH), 125.266 (CH); MALDI-TOF MS (mass *m/z*): 392.49 [M^+]. Anal. calcd for $C_{26}H_{16}S_2$: C 79.55, H 4.11, S 16.34; found: C 79.77, H 4.02, S 16.58.

SI-4 Synthetic routes to 2-TA-AN and 1-TA-AN

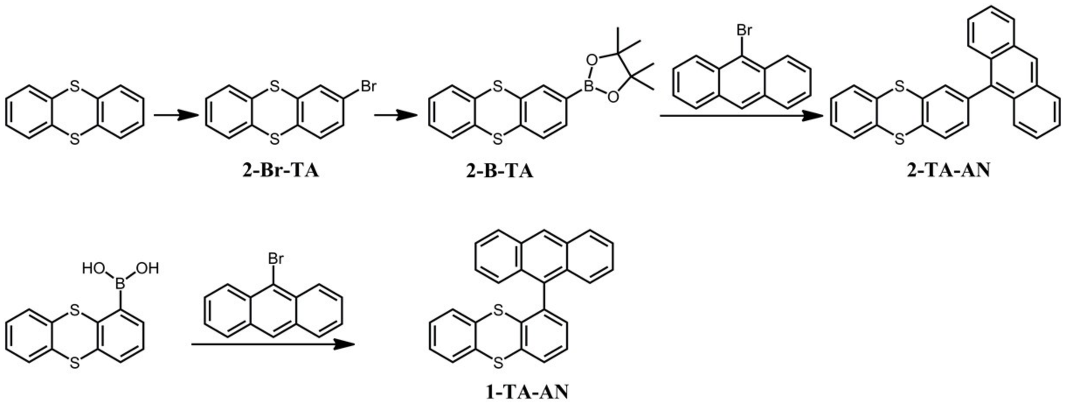

Scheme S1. Synthetic routes to 2-TA-AN and 1-TA-AN.

SII Single crystal X-ray diffraction data

SII-1 General information: Single crystal of 2-TA-AN was prepared by crystallization from chloroform:methanol (3:1, v/v) mixture. Identical crystal of 2-TA-AN could be got whether from THF:methanol (3:1, v/v) mixture or from dichloromethane:petroleum ether (3:1, v/v) mixture. Single crystal of 1-TA-AN was prepared by crystallization from dichloromethane:petroleum ether (3:1, v/v) mixture. Single crystal of 1-TA-AN was also prepared in chloroform:methanol (3:1, v/v) mixture, but only blue crystals were observed. All single crystals were prepared at room temperature. The diffraction experiments were carried out on a Rigaku R-AXIS RAPID diffractometer equipped with a Mo-Kα and control Software using the RAPID AUTO at 293 (±2) ℃. The crystal structures were solved with direct methods and refined with a full-matrix least-squares technique using the SHELXS programs. All the figures of packing structures of crystals were presented using Materials Studio 5.5 Software. All angles and distances in crystals were measured using Mecury 1.4.1 Software.

SII-2 Figures and Tables

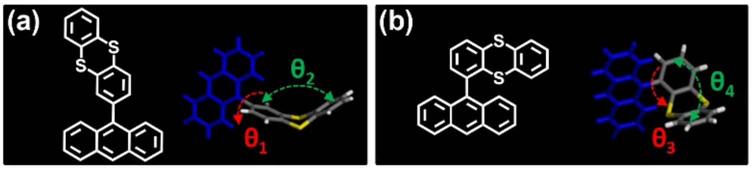

Figure S1. The molecular structures and conformational structures (in crystals) of **(a)** 2-TA-AN (θ_1 = 84° and θ_2 = 126°) and **(b)** 1-TA-AN (θ_3 = 79° and θ_4 = 130°).

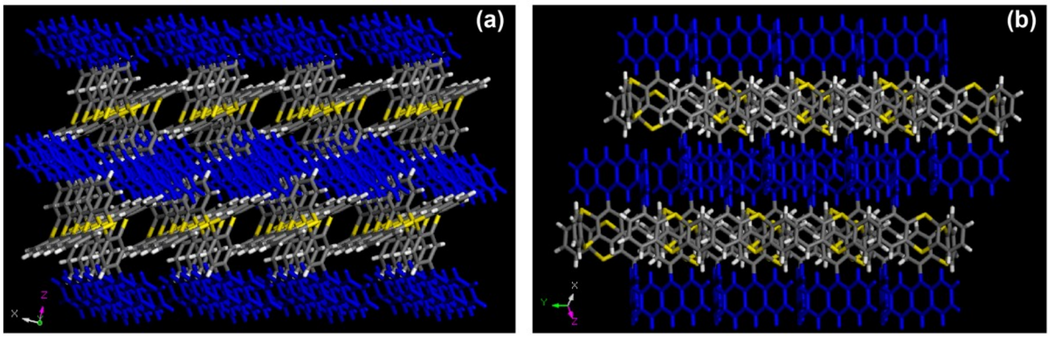

Figure S2. The lamellar stacked structures of **(a)** 2-TA-AN and **(b)** 1-TA-AN crystals with alternative anthracene layer and thianthrene layer.

Table S1. Crystallographic data for 2-TA-AN and 1-TA-AN.

	2-TA-AN	1-TA-AN
crystal colour	yellow	colourless
empirical formula	$C_{26}H_{16}S_2$	$C_{26}H_{16}S_2$
formula weight	392.51	392.51
T [K]	293(2)	293(2)
crystal system	monoclinic	monoclinic
space group	C 2/c	P 21/n
a [Å]	17.080(3)	15.113(3)
b [Å]	11.919(2)	7.7080(15)
c [Å]	19.800(4)	16.178(3)
α [°]	90.00	90.00
β [°]	104.04(3)	94.00(3)
γ [°]	90.00	90.00
V [Å^3]	3910.2(14)	1880.0(6)
Z	8	4
F(000)	1632.0	816.0
density [g/cm^3]	1.333	1.387
μ [mm^{-1}]	0.281	0.292
reflections collected	18204	16091
unique reflections	4429	4255
R (int)	0.0386	0.0356
GOF	1.032	1.051
R_1 [$I>2\sigma(I)$]	0.0423	0.0429
ωR_2 [$I>2\sigma(I)$]	0.1191	0.1055
R_1 (all data)	0.0557	0.0588
ωR_2 (all data)	0.1252	0.1135

SIII Photophysical measurements

SIII-1 General information: UV-vis spectra of solutions and films were recorded on a Shimadzu UV-3100 Spectrophotometer. UV-vis spectra of crystals were recorded on a Lambda 950 UV/Vis/NIR Spectrophotometer, and barium sulfate was used as reflective medium. Crystals were fixed on the surface of compacted barium sulfate, and reflectance spectrum was recorded and transformed into absorption spectrum. Steady-state fluorescence spectra and fluorescence lifetimes were carried out with FLS980 Spectrometer. Quantum efficiencies were measured using an integrating sphere apparatus.

Solutions were placed in 1 cm path length quartz cells, and films were prepared by vacuum evaporation on the quartz plate. Crystals were fixed on the quartz plate in terms of steady-state fluorescence spectra and fluorescence lifetimes.

The radiative decay rate (k_r) and non-radiative decay rate (k_{nr}) were estimated according to Eq. 1. The k_r and k_{nr} of 2-TA-AN crystal were estimated to be 4.89×10^6 s^{-1} and 1.22×10^6 s^{-1} respectively, while the k_r and k_{nr} were 1.00×10^8 s^{-1} and 2.04×10^8 s^{-1} for 2-TA-AN in rigid PMMA matrix, and 2.37×10^7 s^{-1} and 3.55×10^7 s^{-1} for 1-TA-AN crystal. These results demonstrated that non-radiative process was nearly perfectly suppressed by 2 orders of magnitude only in 2-TA-AN crystal relative to that in the doped film.

$$k_r = \frac{\eta_{PL}}{\tau}, \quad k_{nr} = \frac{1}{\tau} - k_r \ldots\ldots (1)$$

SIII-2 Figures and Tables

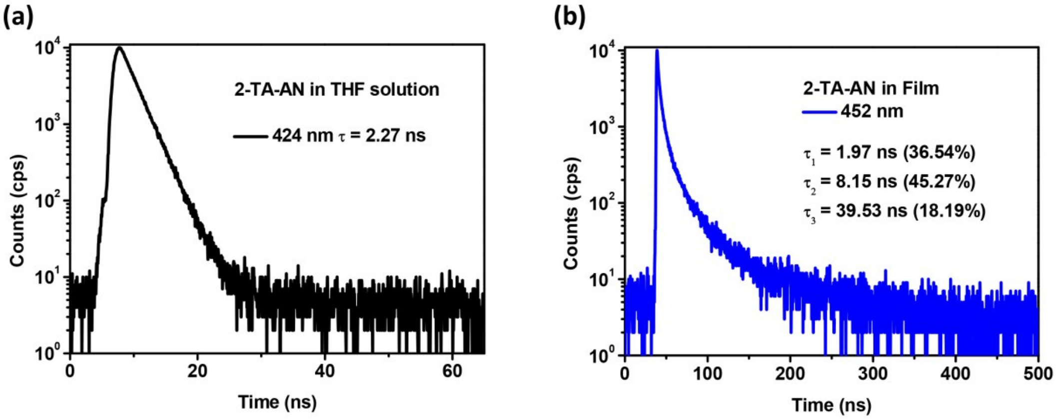

Figure S3. The lifetimes of 2-TA-AN in **(a)** THF solution (1 μM) at the wavelength of 424 nm and **(b)** evaporated film (50 nm) at the wavelength of 452 nm. The detailed lifetime values are shown in figures. The lifetimes of 2-TA-AN in THF solution and evaporated film are far shorter than that of 2-TA-AN crystal.

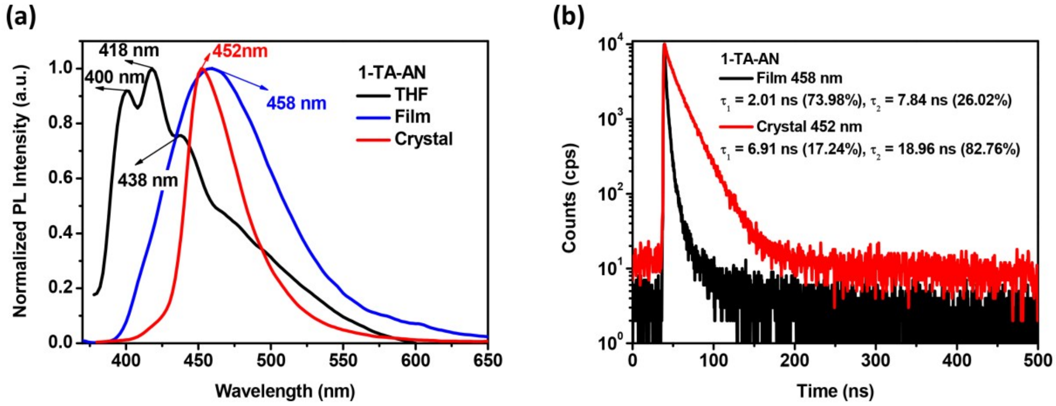

Figure S4. (a) The PL spectra of 1-TA-AN in THF solution (1 μM), evaporated film (50 nm) and crystal. The detailed emission peaks are labeled in figure. 1-TA-AN crystal presents blue emission close to that of evaporated film. **(b)** The lifetimes of 1-TA-AN in evaporated film (50 nm) and crystal. The detailed lifetime values are shown in figure. 1-TA-AN is non-luminous in THF solution and the corresponding decay curve is overlapped with that of IRF, so the lifetime of 1-TA-AN in THF solution is unusable.

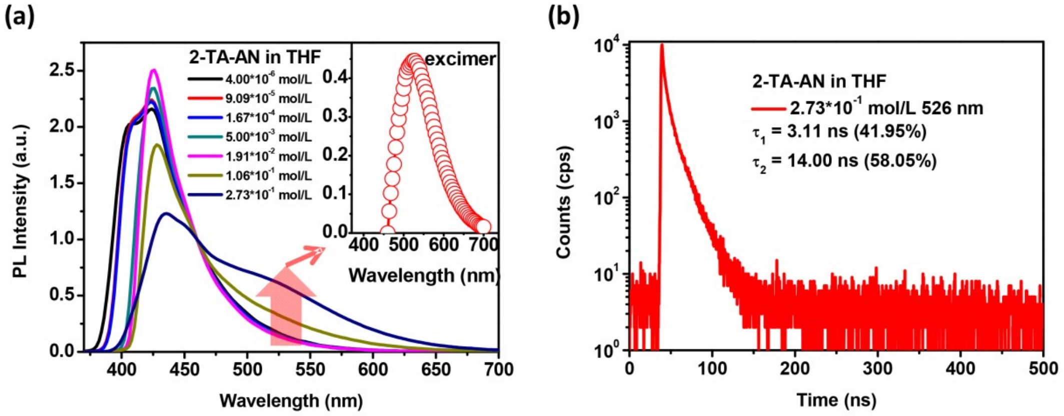

Figure S5. (a) The PL spectra of 2-TA-AN in THF solutions with incremental concentrations from 4.00×10^{-6} to 2.73×10^{-1} mol/L. The PL intensities of 2-TA-AN in THF solutions with incremental concentrations are normalized at wavelength of 460 nm between the regions of former and latter fluorescence. Inset is the resolved excimer spectrum by subtraction of the spectrum of the low-concentration solution (4.00×10^{-6} mol/L) from that of the high-concentration solution (2.73×10^{-1} mol/L). **(b)** The lifetime of 2-TA-AN in THF solution with the concentration of 2.73×10^{-1} mol/L. The detailed lifetime values are shown in figures. The lifetime of 2-TA-AN in THF solution is far shorter than that of 2-TA-AN crystal, probably due to the different surroundings where the excimers are placed.

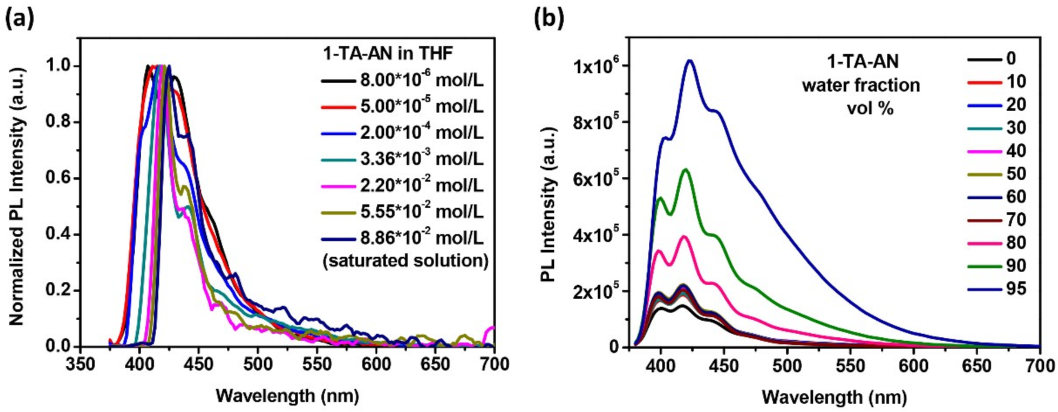

Figure S6. (a) The PL spectra of 1-TA-AN in THF solutions with incremental concentrations from 8.00×10^{-6} to 8.86×10^{-2} mol/L (saturated solution). No new emission band around longer wavelengths is observed. **(b)** The PL spectra of 2-TA-AN in THF:H_2O solutions (10 μM).

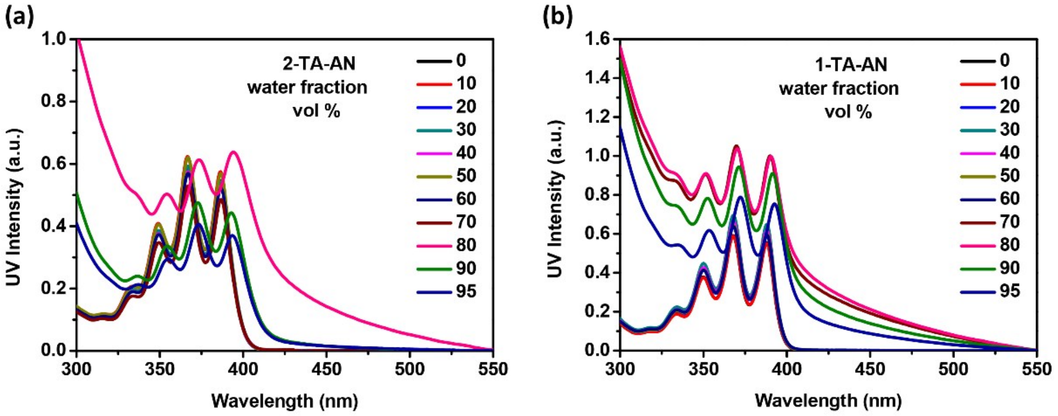

Figure S7. The absorption spectra of **(a)** 2-TA-AN and **(b)** 1-TA-AN in pure THF (10 μM) and THF:H_2O solutions (10 μM). The 0-0 absorption bands are redshifted in the mixture of THF:H_2O (5:95, v/v) relative to that in THF solution.

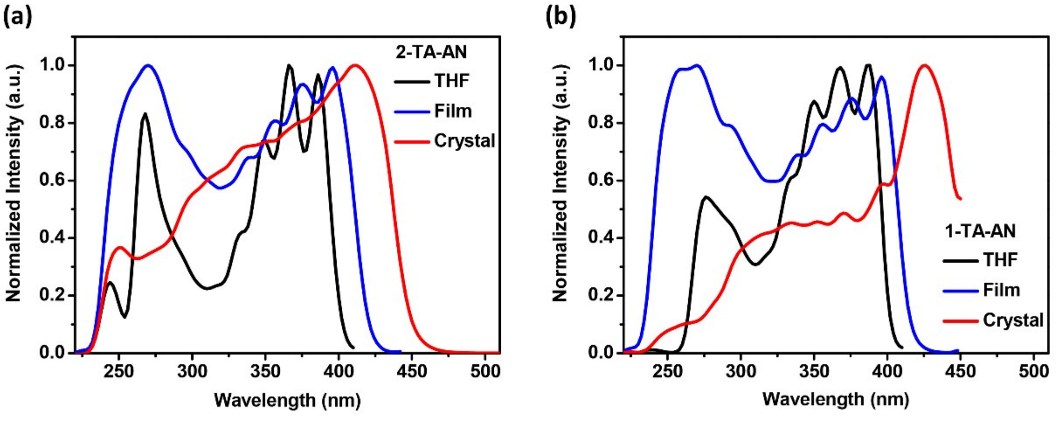

Figure S8. The excitation spectra of **(a)** 2-TA-AN and **(b)** 1-TA-AN in THF solutions (1 μM), evaporated films (50 nm) and crystals. The excitation spectra were recorded at maximum emission peaks. The excitation spectrum of 2-TA-AN crystal is redshifted relative to those in THF solution and evaporated film.

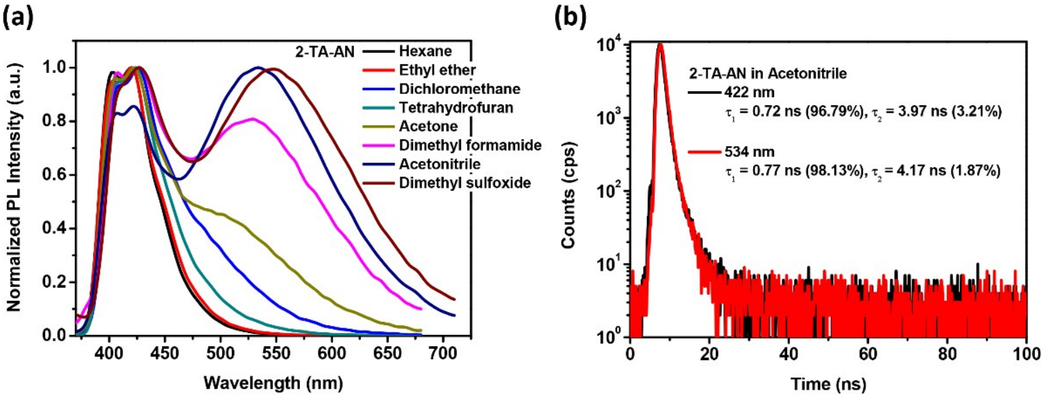

Figure S9. (a) The solvatochromic spectra of 2-TA-AN in the range from low-polarity hexane to high-polarity dimethyl sulfoxide. 2-TA-AN exhibits dual-fluorescence emission in high-polarity solvents. The new emission bands are ascribed to the occurrence of charge transfer (CT). **(b)** The lifetimes of 2-TA-AN in acetonitrile solution (1 μM) at the wavelengths of 422 nm and 534 nm. The detailed lifetime values are shown in figure. The new emission band with CT property possesses short lifetimes.

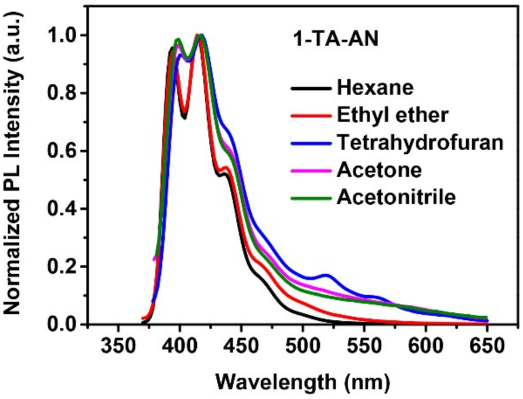

Figure S10. The solvatochromic spectra of 1-TA-AN in the range from low-polarity hexane to high-polarity acetonitrile. 1-TA-AN shows trailing PL spectra in high-polarity solvents which is ascribed to faint CT emission, although no obvious emission band is observed at long wavelength.

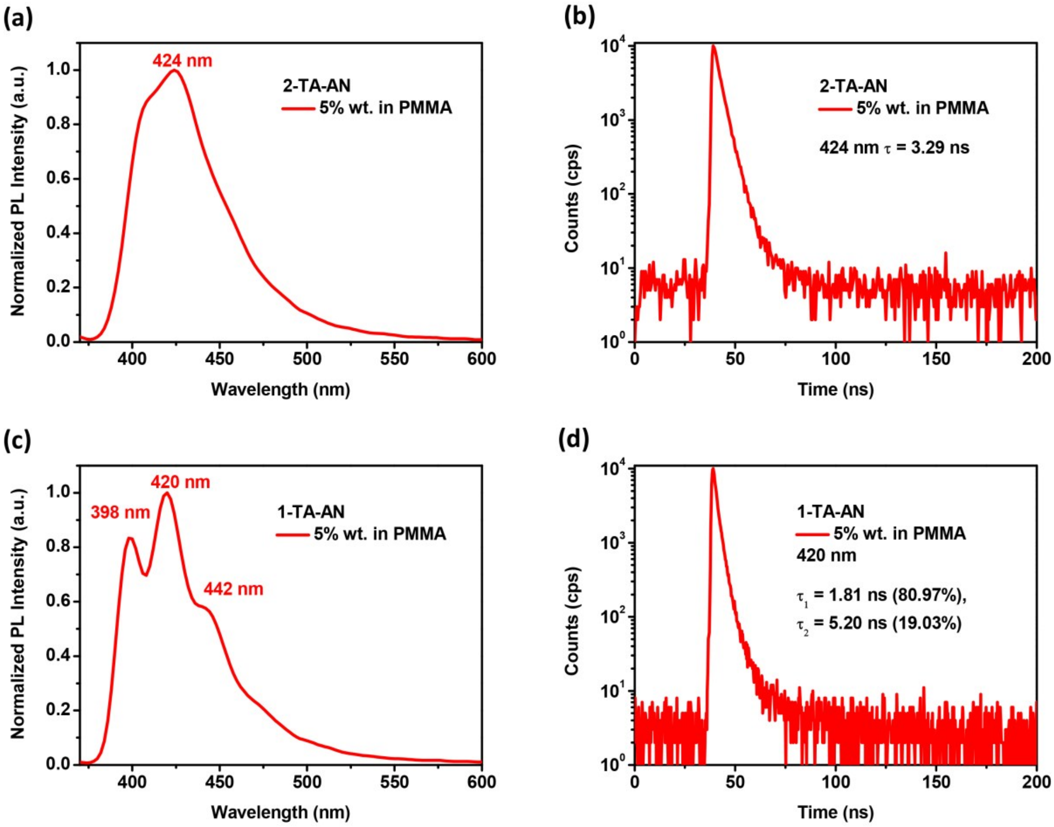

Figure S11. (a) The PL spectra of 5% weight of 2-TA-AN in PMMA. **(b)** The lifetimes of 5% weight of 2-TA-AN in PMMA. **(c)** The PL spectra of 5% weight of 1-TA-AN in PMMA. **(d)** The lifetimes of 5% weight of 1-TA-AN in PMMA. The detailed lifetime values are shown in figure.

SIV Theoretical calculation

SIV-1 General information: All the density functional theory (DFT) calculations were carried out using Gaussian 09 (version D.01) package on a PowerLeader cluster.[2] The density functional theory (DFT) and time-dependent DFT (TDDFT) were carried out for the geometry optimization and the frequency calculation of ground state and excited state at the level of B3LYP/6-31G(d, p), respectively. The absorption and emission properties were obtained using TD-M06-2X/6-31G(d, p) at the ground state and excited state geometries, respectively. In order to examine the nature of electronic transitions for excited-states, natural transition orbitals (NTOs) are evaluated with the dominant “particle”-“hole” pair contributions and the associated weights.

SIV-2 Figures and Tables

Molecules	Ground state (S_0)	Excited state (S_1)
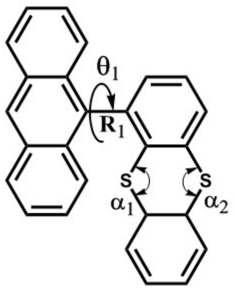 1-TA-AN	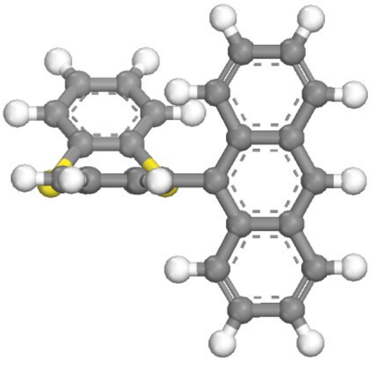	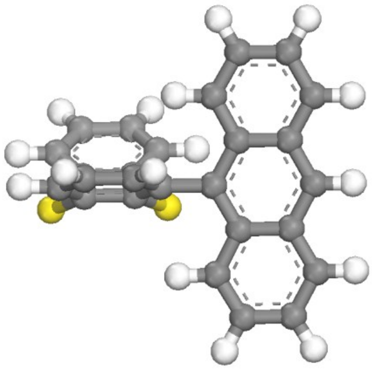
Optimized geometry parameters	R_1=1.4992Å; θ_1=89.09˚; α_1=101.54˚ α_2=101.40˚	R_1=1.4947Å; θ_1=101.97˚; α_1=101.58˚ α_2=101.51˚
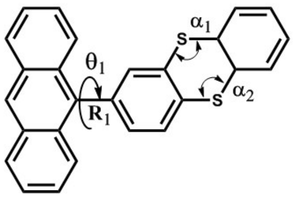 2-TA-AN	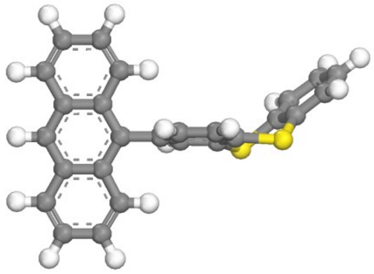	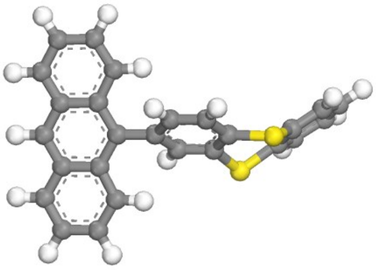
Optimized geometry parameters	R_1=1.4974Å; θ_1=82.39˚; α_1=101.50˚ α_2=101.47˚	R_1=1.4713Å; θ_1=53.74˚; α_1=102.14˚ α_2=102.28˚

Figure S12. The ground state and excited state geometries of 1-TA-AN and 2-TA-AN.

Molecules	HOMO	LUMO
1-TA-AN	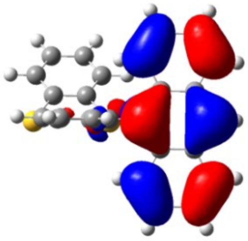 E (HOMO) = -4.07 eV	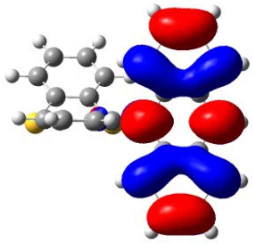 E (LUMO) = -1.32 eV
2-TA-AN	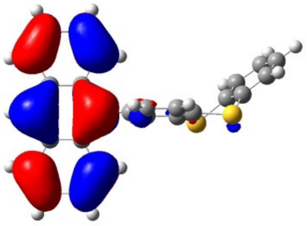 E (HOMO) = -4.10 eV	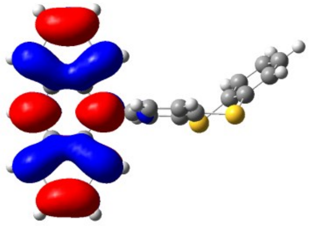 E (LUMO) = -1.35 eV

Figure S13. HOMO and LUMO of 1-TA-AN and 2-TA-AN. HOMO and LUMO are almost located on anthracene moiety, whether for 1-TA-AN or for 2-TA-AN.

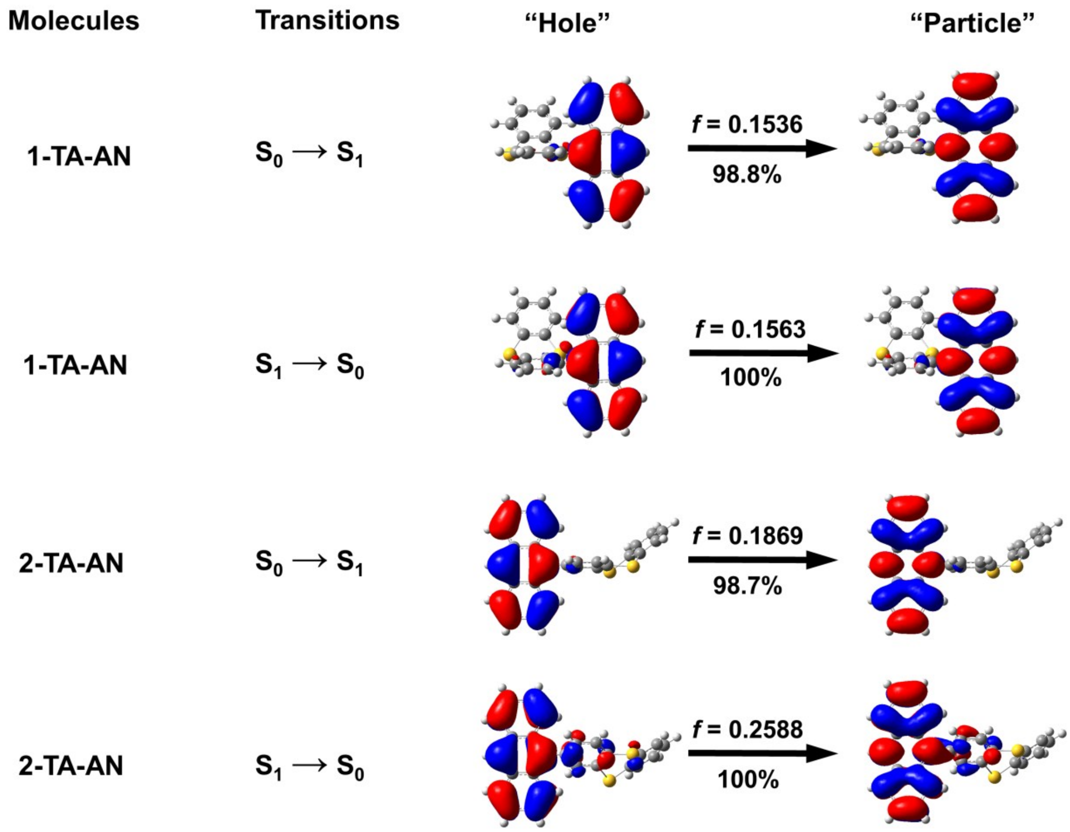

Figure S14. Natural transition orbital (NTO) of S$_0$→S$_1$ and S$_1$→S$_0$ in 1-TA-AN and 2-TA-AN.

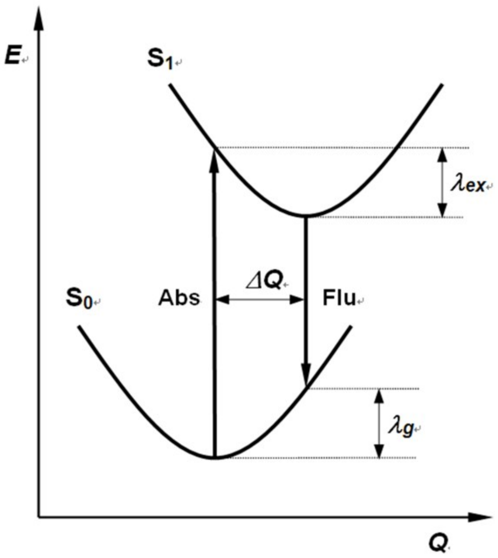

Figure S15. The calculation details of relaxation energy using the four-points approach. Here, the relaxation energies λ_{ex} and λ_g are along the potential energy surfaces of excited state (S$_1$) and ground state (S$_0$) respectively; the vertical axis is the energy E, and the horizontal axis is the normal mode displacement Q.

Table S2. The vibrational relaxation energy of 2-TA-AN and 1-TA-AN along the excited state potential energy surface by DUSHIN.

Frequency (cm^{-1})	2-TA-AN	Frequency (cm^{-1})	1-TA-AN
	λ_i (cm^{-1})		λ_i (cm^{-1})
23	448.9	13	100.5
30	476.9	30	3.2
41	163.3	43	1.9
59	82.4	53	27.4
83	6.5	75	9.7
108	5.4	97	0.2
123	77.2	112	2.9
136	52.7	129	1.3
160	185.7	151	23.2
180	0.1	186	0.5
204	139.3	205	3.8
227	0.3	233	0.7
241	25.1	240	2.1
260	3.4	261	1
276	43.6	263	1.7
303	1.3	289	1.2
317	9.1	307	0.3
346	24.4	333	1.2
359	20.3	351	0
393	92.3	394	138.6
405	0.1	402	3.9
409	0.1	405	1.3
411	0.2	413	9.2
437	23.8	432	0.2
441	23.1	440	4
456	3	468	0.3
480	3.4	486	0.8
495	0.3	500	0
511	0.1	512	0.2
516	2.7	514	0
522	0.7	517	0.1
540	1.3	528	0
553	0	555	0.6
599	0.2	596	0.1

615	0	617	3.1
633	2.9	622	0.4
637	7.2	628	7.4
673	0.1	666	0.2
673	5.8	674	0
689	1.3	709	0.6
718	1.1	719	6.4
718	1.4	720	2.5
723	0.1	725	0
731	0	731	0
738	0.6	735	0.6
746	0.2	737	0.3
755	0	752	0.3
758	4.9	764	0.9
767	0	767	0
813	0	798	0.1
839	0.3	807	0.1
852	1.2	845	0
858	4.9	854	5.1
877	0.2	874	0
878	0	877	0
880	0.1	878	0
903	0.3	895	0
908	0.3	900	0
919	3.7	916	0
939	0.9	939	0
947	0	943	0
950	0.2	945	0
953	0	953	0
963	1.7	967	1.1
974	2.7	979	0
991	0	990	0
1037	1	1047	0
1057	0.9	1059	0.9
1059	0.3	1061	23.9
1066	36.9	1063	3.8
1074	0	1068	0.1
1106	0	1100	0
1123	0.3	1119	0.6
1139	1.6	1131	0.1
1145	0.2	1140	0
1154	0	1153	0
1175	0	1171	2
1182	0	1181	0.4
1188	129.9	1190	73.9
1191	5.4	1190	33.9
1197	4.6	1196	0.2
1220	0	1220	0
1275	0.1	1230	2.2
1278	0	1277	0.2
1283	0.4	1282	0
1294	8.9	1289	3.9
1305	0.3	1306	0
1307	0.2	1311	0
1333	0.4	1335	0
1337	0	1346	1.2
1354	18.9	1356	0
1392	1.1	1400	0
1406	781.1	1422	653.2
1419	8.8	1424	145.6
1437	0.1	1438	0.3
1466	0	1463	1.2
1467	0	1466	0
1475	6	1471	3.2
1485	0.1	1478	4
1499	0.8	1492	0
1537	186.9	1537	0.2
1541	10.5	1541	207.3
1553	5.2	1558	1.3
1563	0.1	1587	0.4
1587	0.5	1592	9.8
1590	79.2	1602	195
1606	151.4	1607	81.3
1615	2.5	1615	2.3
1624	30.5	1621	2.6
1630	9.3	1628	0
3170	0	3169	0.1
3179	0	3179	0
3180	0.1	3180	0.1
3189	0	3187	0
3190	0	3189	0
3191	0	3190	0
3194	0.1	3191	0
3197	0	3197	0
3206	0	3203	0
3207	0.2	3205	0.1
3207	0.2	3205	0
3209	0.1	3207	0.1
3214	0.1	3212	0

3215	0.1	3213	0
3223	0.1	3217	0
3225	0.2	3218	0
	λ_{ex} = 3444.9 (427 meV)		λ_{ex} = 1826.6 (227 meV)

Molecules	Frequency (cm^{-1})	Front view	Side view
1-TA-AN	13	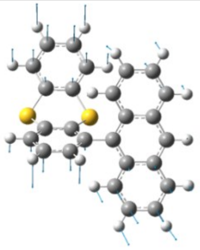	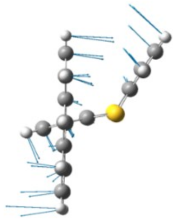
2-TA-AN	23	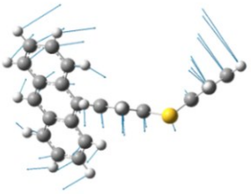	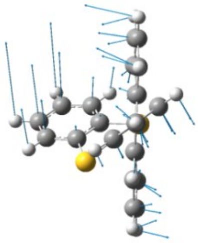
	30	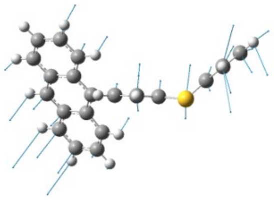	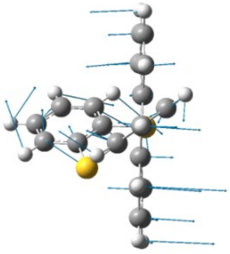
	41	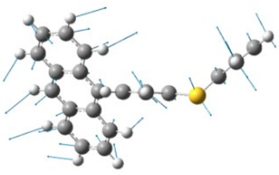	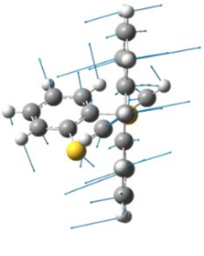

Figure S16. Vibrational normal modes of 1-TA-AN and 2-TA-AN at excited state. The relaxation energies (Λ) could be obtained through the summation of all vibrational normal-mode relaxation energies in excited state (λ_{ex}). Particularly, Huang-Rhys (HR) factors for every normal mode were also estimated according to Eq. 1, using DUSHIN program developed by Reimers.[3]

$$\Lambda = \sum_i \lambda_i = \sum_i \frac{1}{2} k_i \Delta Q_i^2 = \sum_i \hbar\omega_i S_i \qquad (1)$$

Where, ΔQ_i represented the rigid displacement along the ith normal mode for the equilibrium geometries of excited states. k_i and ω_i were the corresponding force constant and circular frequency for the ith normal mode, respectively. S_i was the HR factor for the corresponding frequency mode.

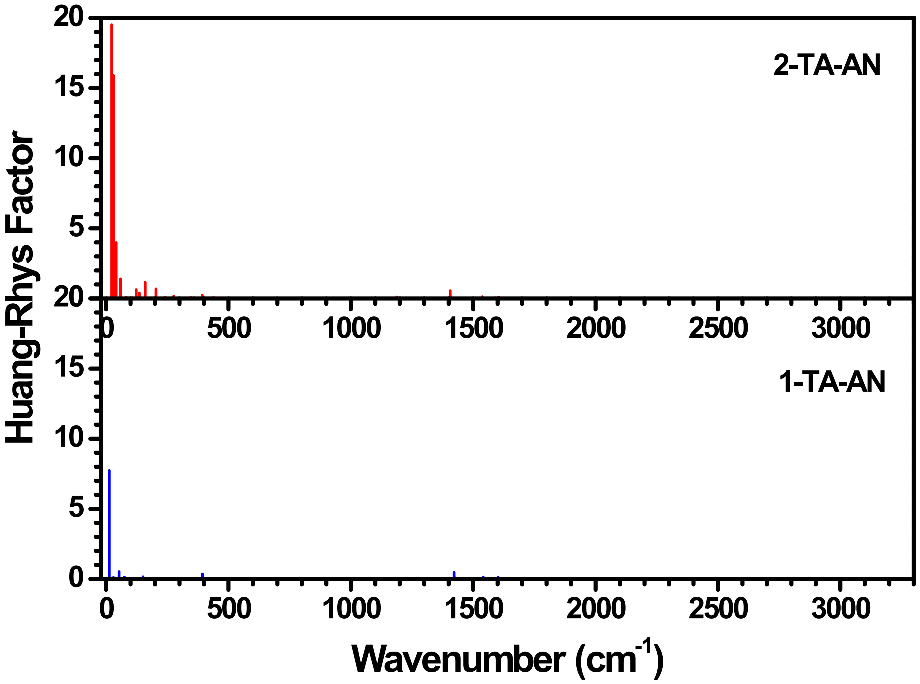

Figure S17. Huang-Rhys Factors of normal modes of 2-TA-AN (top) and 1-TA-AN (down) excited state. The vibrational modes with maximal HR factors all fall in the low-frequency region for both 2-TA-AN and 1-TA-AN, corresponding to intramolecular twisting rotation between anthracene and thianthrene moieties, as well as C–S–C angle bending vibrations of thianthrene.

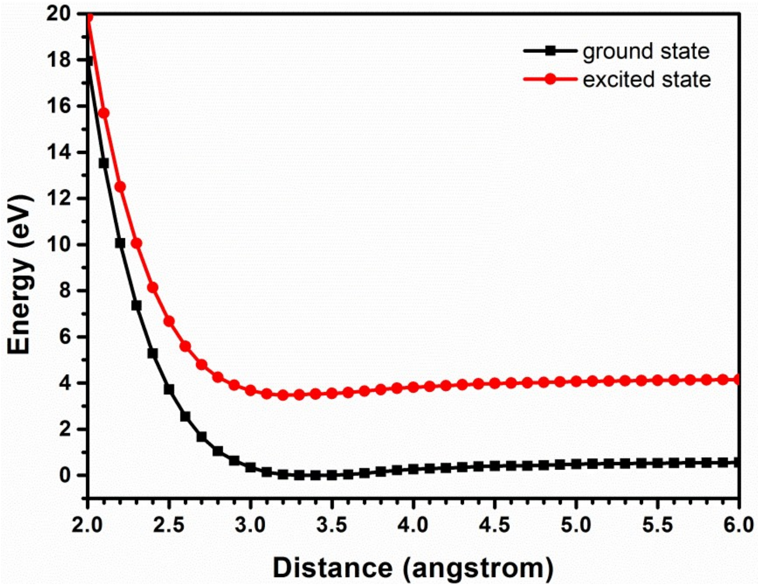

Figure S18. Schematic diagram of the relationship between a dimer of 2-TA-AN in the ground state (S_0) and an excimer in the excited state (S_1). 2-TA-AN dimer undergoes a relaxation energy of 0.051 eV at the excimer excited state and 0.035 eV along the dimer ground state after the excitation of monomer in the ground state, corresponding to a decreased interplanar separation from 3.4 Å to 3.2 Å to form the excimer of 2-TA-AN. The PESs as a function of interplanar distance (2.0 ~ 6.0 Å) between anthracene dimer were obtained using TD-M06-2X(GD3)/6-31G(d, p) at the ground state and excited state, respectively.

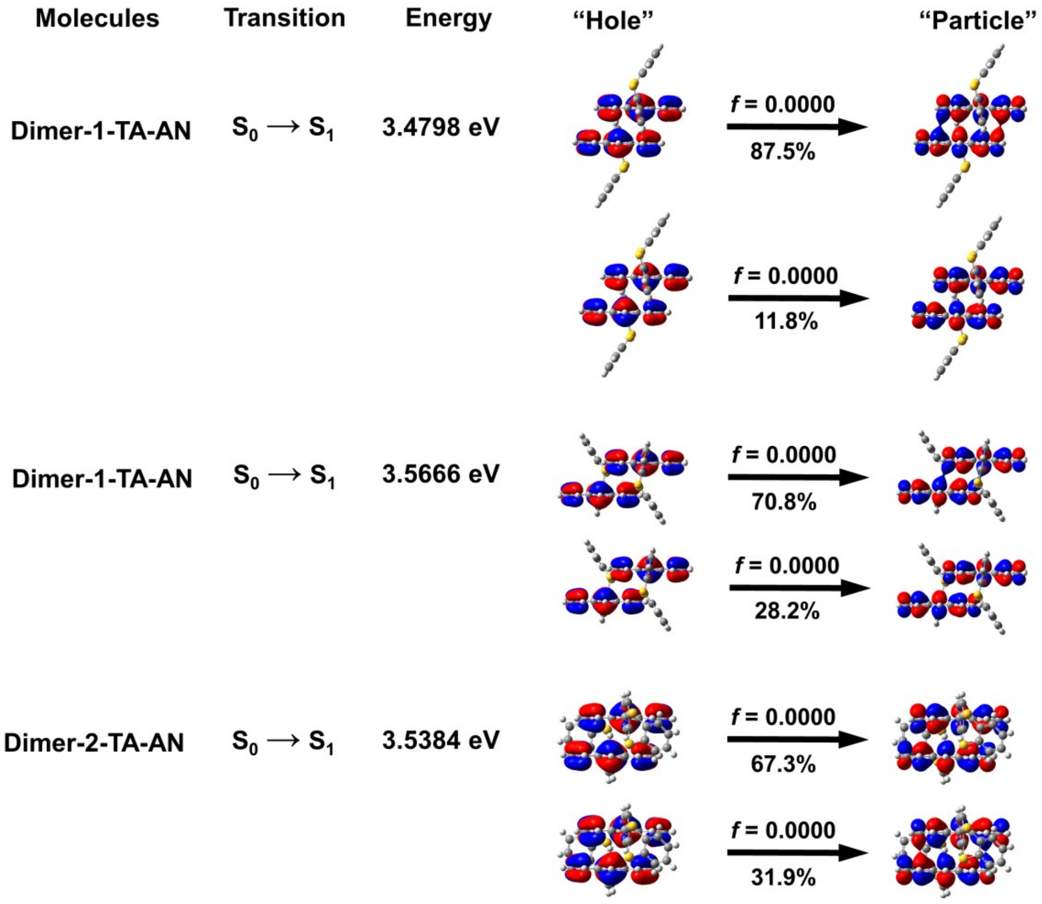

Figure S19. Natural transition orbital (NTO) of $S_0 \rightarrow S_1$ for 1-TA-AN and 2-TA-AN dimers, together with vertical transition energy, oscillator strength and the weight of hole-particle pair.

Table S3. Absorption and emission properties of 1-TA-AN and 2-TA-AN in vacuum gas phase by TDDFT-M06-2X/6-31G (d, p) at the optimized geometries by B3LYP/6-31G (d, p).

Molecules	Abs/Emi	Electronic transition	λ_{cal} (nm)	Oscillator strength (f)	λ_{exp} (nm) in Hexane
1-TA-AN	Abs	$S_0 \rightarrow S_1$	347.05	0.1536	385,365,348,331
	Emi	$S_1 \rightarrow S_0$	404.99	0.1563	471,437,415,394
2-TA-AN	Abs	$S_0 \rightarrow S_1$	346.25	0.1869	384,364,347,330
	Emi	$S_1 \rightarrow S_0$	414.34	0.2588	420,404

SV Reference

[1] H. Morita, Y. Oida, T. Ariga, S. Fukumoto, M. C. Sheikh and T. Fujii, T. Yoshimura, *Tetrahedron* 2011, **67**, 4672.

[2] M. J. Frisch, G. W. Trucks, H. B. Schlegel, G. E. Scuseria, M. A. Robb, J. R. Cheeseman, G. Scalmani, V. Barone, B. Mennucci, G. A. Petersson, H. Nakatsuji, M. Caricato, X. Li, H. P. Hratchian, A. F. Izmaylov, J. Bloino, G. Zheng, J. L. Sonnenberg, M. Hada, M. Ehara, K. Toyota, R. Fukuda, J. Hasegawa, M. Ishida, T. Nakajima, Y. Honda, O. Kitao, H. Nakai, T. Vreven, J. A. Montgomery, Jr., J. E. Peralta, F. Ogliaro, M. Bearpark, J. J. Heyd, E. Brothers, K. N. Kudin, V. N. Staroverov, R. Kobayashi, J. Normand, K. Raghavachari, A. Rendell, J. C. Burant, S. S. Iyengar, J. Tomasi, M. Cossi, N. Rega, J. M. Millam, M. Klene, J. E. Knox, J. B. Cross, V. Bakken, C. Adamo, J. Jaramillo, R. Gomperts, R. E. Stratmann, O. Yazyev, A. J. Austin, R. Cammi, C. Pomelli, J. W. Ochterski, R. L. Martin, K. Morokuma, V. G. Zakrzewski, G. A. Voth, P. Salvador, J. J. Dannenberg, S. Dapprich, A. D. Daniels, Ö. Farkas, J. B. Foresman, J. V. Ortiz, J. Cioslowski and D. J. Fox, *Gaussian 09, Revision D.01*, Gaussian, Inc.: Wallingford CT, USA 2009.

[3] J. R. Reimers, *J. Chem. Phys.* 2001, **115**, 9103.